The Optical and Electronic Design of a Hybrid Digital/Optical Correlator System

Philip M. Birch, Frederic Claret-Tournier, David Budgett, Rupert Young, Chris Chatwin.

School of Engineering and Information Technology
University of Sussex
Brighton
East Sussex
BN1 9QT
United Kingdom
Tel: +44(0)1273 872572
Fax: +44(0)1273 690814
e-mail: p.m.birch@sussex.ac.uk

Abstract

The design of a digital-optical hybrid correlator is detailed. The optical Fourier transform lens design and mechanical lens housing are detailed as well as the video rate fast Fourier transform digital signal processing (DSP) hardware and overall electronic control. Example results using several different filters and modulation techniques are described.

Keywords Correlator, Optical Design, Digital Design, Image recognition

Introduction

Optical correlation enables the rapid identification of targets within an input signal. This is due to the inherent Fourier transforming property of an optical lens system, together with the capability of performing a complex multiplication between a holographically

recorded function and a coherent wavefront [1]. However, for the recognition of a 3-D object unconstrained in scale, rotation and orientation, many reference template searches may be required for recognition. The number of template filters that can be stored in thin holographic films is limited so it is now common to use a temporal multiplexing filter technique employing spatial light modulators (SLM)[2-5]. However, to realise the full programmable flexibility required, an effective electronic control and data interface must be implemented between the optical processor and a digital computer [6].

Conventional modern 4-f correlator systems typically consist of the following: An input camera, which is controlled by a computer, is used to record the input signal. The input signal is digitised and displayed on an intensity modulating liquid crystal SLM. The SLM is coherently illuminated with a laser and this signal is optically Fourier transformed to the frequency plane via a lens system. In the frequency plane the signal is mixed with pre-designed template filters represented on a second SLM and this new signal is again optically Fourier transformed, and the correlation peak is detected by a second camera. The peak then gives an indication of correlation between the input signal and filter.

To perform unconstrained pattern recognition, it is generally necessary to perform several template searches per input signal. There is therefore a difference in the frame rate requirements of the input and template/peak detection sections of the correlator system. The hybrid correlator described below uses this fact to its advantage.

The conventional all optical correlator system often has many of the limitations that are briefly described below:

- Input SLM choice. There are problems associated with low signal to noise ratio, slow speed, phase noise, and dynamic range.
- Physical size. For practical applications we wish limit the physical size to fit inside a PC on an expansion board. Conventional 4f correlators tend to be large and require a complex optical design to decrease their size making them difficult to place inside a PC.

- Physical robustness and alignment. The current trend of SLM design is towards smaller pixels. SLMs are available with 7μm pixel pitches. The zeroth frequency pixel of the filter template SLM must be lined up to the DC of the input signal to maintain a high quality correlation spot. The small pixel pitch of the SLM leads to a very difficult mechanical design problem when the correlator is subjected to environmental perturbations.
- The laser source must illuminate the input SLM with uniform intensity across its field. Conversion from the Gaussian beam profile of a laser to a flat profile is non-trivial.

This paper will discuss the design and construction of a hybrid correlator design that utilises the accuracy of a digital fast Fourier transform (FFT) algorithm and the high-speed capabilities of an optical Fourier transform for the filter search.

Basic System Design

A hybrid correlator, constructed as shown in figure 1, realises a high speed and programmable recognition system based on image correlation. This method overcomes the limitations of conventional correlators listed above by using digital electronics to perform the first leg of the correlation and high-speed optics to perform the fast template search. The system consists of five basic sections:

- a digital video camera capturing a 512x512 image at 40 frames per second rate,
- a signal processor array performing the FFT algorithm and a complex multiplication with the reference templates,
- an SLM which acts as the interface between the electronics and optics,
- an optical system to perform an Fourier Transform of the frequency plane product,
- a high frame rate camera to detect the correlation peak.

The input scene is captured through a slow, but high-resolution camera, as in a conventional correlator (CCD1 in figure 1). This data, instead of been displayed on an SLM and optically Fourier transformed, is digitally Fourier transformed using a real to complex FFT implemented on Digital Signal Processors (DSP) chips. This complex data is then mixed electronically using a 2D multiplicative function with pre-designed template filters. This data is displayed on an SLM, which is coherently illuminated with a beam expanded laser diode, and this signal is optically Fourier transformed with a lens. This intensity pattern is captured on a low resolution, but high speed CCD camera (CCD2). The intensity data is then sent to a high speed DSP where is the signal is peak detected, and the results are returned to the host computer.

This arrangement exploits the asymmetry in the processing time requirements between the initial Fourier transform on the input image (~40ms), performed only once for each input frame, and the template matching operation of the stored reference images, which may be addressed many times per FFT to achieve complete recognition. Due to a large number of references, the template matching is to operate ideally at a speed of at least two orders of magnitude faster than the FFT process.

Since there is no input SLM with this system, the problems associated with all optical correlators have been removed. The first leg of the system is performed electronically so there is high dynamic range and a high signal to noise ratio. The physical size has been reduced due to the electronic systems and a much simpler optical system. Since there is no requirement to align the system so that in the input Fourier transform's DC term is aligned within one SLM pixel, the over all system alignment tolerances have been greatly reduced, which in turn improves the overall robustness of the system. Finally, since the frequency plane is now been illuminated by the laser, a Gaussian intensity profile is not so much of problem. Indeed, the beam profile can be advantageous since it provides a high frequency apodisation.

2D FFT: Mathematical background

The Discrete Fourier Transform (DFT) of an *N*-point discrete signal *h(i)* is defined by:

$$H(k) = \sum_{n=0}^{N-1} h(n) W_N^{nk} \qquad [1]$$

where $W_N = e^{-j2\pi/N}$ and $0 \le k \le N-1$. Direct DFT computation requires $O(N^2)$ arithmetic operations, while the Fast Fourier Transform (FFT) algorithm requires only $O(N \cdot \log_2 N)$ arithmetic operations. The 2D FFT is simply calculated by performing an FFT on the row data, then on the column data. The number of computations required is therefore:

$$Time_{N\times N} = 2 \cdot N \cdot O(N \cdot \log_2 N) \approx O(N^2 \cdot \log_2 N) \qquad [2]$$

However, in the hybrid correlation system, the incoming 2D image from the CCD camera represents a grey scale image consisting of real only data. According to the properties of the Fourier transform, the matrix resulting after the first 1D FFT is distributed with complex conjugate symmetry in the *N*-rows about the Nyquist frequency, *N*/2. Consequently the 1D FFT calculation on the *N*-columns is only carried out on half of the total columns (*N*) while the other half of the data for the final 2D FFT can be obtained by the complex transpose. This can be expressed as:

$$H_{real}(i,j) = H_{real}(N-i, N-j) \;\; and \;\; H_{imag}(i,j) = -H_{imag}(N-i, N-j), \;\; \forall i, j \in \left[0; \frac{N}{2} - 1\right] \qquad [3]$$

Therefore, the timing to implement the 2D FFT at *N*-points can be written as:

$$T_{2D-N} = O(N \cdot \log_2 N) + T'_{transp} \qquad [4]$$

where T'_{transp} denotes an execution time for handling the complex transpose, requiring a data transfer between the multi-processors.

Architecture for parallel processing of the 2D Fourier transform

The key point for consideration in a digital system for implementing a 2D FFT, the template matching, complex multiple, and the interface for a digital camera, is the optimal combination of software and hardware. In the specific application of the hybrid correlator, a 2D FFT is to be performed every 40ms for a 25 Hz CCIR standard frame rate, so an optimised hardware architecture is demanded to support the given level of performance.

The Super Harvard Architecture Computer (SHARC) Analogue Devices ADSP-21060 has been chosen to realise the real-time digital hybrid correlator, since, unlike the majority of DSP solutions, the SHARC device is explicitly designed for implementation as a parallel array. Furthermore, the associated development system such as code libraries, compiler or debugger are mature products, so many compatible interfaces have been extensively developed. The SHARC processors have the provision for six external high-speed data links.

Figure 2 shows the electronics systems layout for the hybrid correlator. CCD1 is a 512x512 DALSA camera with a 25Hz frame rate. A field programmable gate array (FPGA) was programmed to directly control the camera and handle the data. This is passed through a FIFO (first in, first out) to the first SHARC (SHARC1). The FIFO acts as an electronic buffer that simplifies the connection between the FPGA and the SHARCs. Eight processors are arranged in two groups of four (SG1 and SG2). SHARC1 acts as a data routing controller. The first four perform an FFT on the data in 75ms. The next CCD frame is then sent to SG2 that again performs a 75ms FFT. This is then equivalent to a sub 80ms FFT, although there is a 40ms pipeline delay. Alternative architectures such as six meshed processors have also been tested but the two groups of four gave the best performance and so this was used. Another two SHARCs, SHARC2

and SHARC3, then perform the template multiplication. The data is sent in turn to SHARC4 that acts as the SLM controller via another FIFO and FPGA2.

The SLM can be controlled by one of two methods: other the ISA bus or via its DALSA camera input. Since the ISA bus is too slow, FPGA2 was programmed to mimic the output for a DALSA camera. This enables a frame rate of 915Hz for the SLM.

Also shown in figure 2 is the correlation spot capture and processing system. As in CCD1, CCD2 is controlled by a SHARC processor, which uses a FIFO and FPGA3 as the electrical interface. SHARC5 performs the peak detection and returns the result to the host PC.

This arrangement provides for a video rate FFT, and high speed electronic mixing. There is still however a requirement for the second leg to be performed optically since this frame rate is to slow to search many templates per digital FFT input if the second leg of the system was performed digitally. The frame rates of each component are summarised in table 1.

SLM

A Boulder Nonlinear Systems (BNS) analogue ferroelectric (AFLC) SLM is used. It has 128x128 pixels and a frame rate of 915Hz. The device is capable of modulating along the real axis, in an analogue and bipolar (i.e. positive and negative) manner.

At 670nm the SLM pixels are equivalent to approximate have-wave plates with an electronically controllable optical axis. Any deviation from π retardance results in an optical transmitted efficiency loss. The SLM is placed behind a polarising beam splitter. The input polarisation state is linear and aligned to bisect the maximum angles of the optical axes achievable by the SLM. If the optical axis of the SLM pixel is at angle θ to the plane of polarisation of the incident light, the reflected light will have been rotated by angle 2θ. The polarising beam splitter is then used to select the polarisation component

orthogonal to the incident polarisation and hence gives an amplitude modulation of the beam. If the optical axis of the pixel is rotated -θ, the outgoing light will be rotated in the opposite direction leading a negative amplitude modulation compared to the positive θ example. This allows analogue modulation along the real axis in both positive and negative directions.

The advantage of such an SLM is that it allows for several modes of operation: binary phase, real axis modulation, amplitude modulation, and limited analogue phase modulation.

Binary Correlation

The fastest implementation of the correlator system is when a binary SLM is used. This can be a conventional FLC or the newer analogue FLC (AFLC) operated in binary mode. Binary correlation only requires the phase of the data to represented as either -1 (for zero phase) or 1 for (π phase). Most of the complex data calculated by the FFT can then be discarded. Only the sign of the real component is needed. The same operation is carried out on the template data (offline) and the data to written to the SLM is calculated using an exclusive NOR operation (or an exclusive OR which gives the same result when placed on the SLM because the absolute phase is not important). This simple bitwise operation can be carried out extremely fast, although at the expense of the accuracy of the correlator, which has been reduced to a binary-binary phase only filter.

Complex Correlation

The use of an AFLC SLM offers the possibility of several interesting encoding techniques. As demonstrated in references 7 and 8, the SLM is capable of performing full complex modulation with full phase and amplitude control to 8-bit resolution. In this configuration, each pixel of the device can modulate along the real axis, both in a positive and negative direction with 256 grey levels. Since negative modulation can be achieved, a two-element macro-pixel can be used to represent a complex number. One element

represents the real data and one the imaginary. Full complex modulation is achieved off axis, in a direction where there is a $\pi/2$ phase lag between the two pixels. In addition, every second macro-pixel must be negated to remove the π phase lag that would otherwise occur between the adjacent real components. Obviously, the filter calculation now requires a complex multiplication that is not as fast as a simple XOR operation but can neither the less be rapidly performed at a reduced bit resolution with fixed point arithmetic.

Optical System Design

The hybrid correlator is designed to fit inside a PC. The optical system design must therefore be sufficiently compact to fit onto an aluminium plate measuring 210mm by 110mm. The components to be mounted on this are: the laser module, a beam expander, the SLM, and the Fourier transform lens. A high frame rate 128x128 pixel DALSA camera was chosen as the peak detection camera. Since these cameras are physically bulky there is no room on the board for the camera. For this reason an image transfer fibre optic bundle was used so the camera can be mounted elsewhere in the PC. The optical layout of the system is shown in figure 3. A temperature controlled laser diode is used as the light source, which is collimated and beam expanded. Two beam splitters are shown in figure 3. The first beam splitter is for the illumination of the SLM and the second is to allow an additional CCD camera to be added. The additional camera has not yet been implemented; but it will be a high-resolution camera running at a slower frame rate. This camera will be used to provide a higher quality image of the correlation plane.

The lens L1 performs two tasks: the collimation of the beam expander system and the first part of the FT system. For mechanical restrictions, a 15mm gap is left between the SLM and L1. Because the aperture stop is placed on the surface of the SLM, from an aberration point of view, the larger this gap is, the higher the off-axis rays are at the following lenses, and the more difficult to correct the off-axis aberrations. Therefore, this gap should be kept at a minimum. Leaving a space (0.5mm) between L1 and the first beam splitter permits the use of the spacings to compensate manufacturing errors. It is

easy to control lens spacings very precisely by the use of precision rings as spacers. These spaces should be as small as practical to make a compact system.

Because of the small area available, the Fourier transform lens is the most problematic to design. The required focal length of the lens to match the pixelation of the SLM and camera is given by

$$f = \frac{N_2 D_2 D_1}{\lambda} \qquad [5]$$

where N_2 is the number of pixels in each row of the CCD, D_2 is the pixel size of the CCD array, D_1 is the pixel size of the SLM and λ is the wavelength. For our components, N_2= 128, D_2=16μm, D_1=40μm and λ = 670nm, which corresponds to a focal length of 122 mm. The required f-number is then *f*/16.85 for CCD1.

For this optical FT system, the phase error caused by placing the SLM off the front focal point of the FT lens is not considered because of the use of intensity detectors, and the FT lens can be considered as a photographic objective with the optical stop at the surface of the SLM. Therefore, the angle field of view, ω, of the optical system is determined by the aperture of the CCD array and the focal length of the first leg (or the second leg) of the FT lens: $\omega = \arctan(y/f)$, where *y* is half of the diagonal distance of the CCD array and *f* is the focal length of the first leg of the FT lens. Substituting the corresponding data into the above equation, the angle field of view is ω=1.70°.

FT Lens Design

No chromatic aberration correction is necessary since the system uses a diode laser source with a wavelength of 670 nm. Other aberrations should be all corrected for a FT lens. As the objective of the beam expander, the on-axis aberrations should be well corrected in L1. It is reasonable to use L2 to balance the off-axis aberrations since the field of view is small. A doublet is suitable for L1, whose focal length is chosen as 55mm with a beam diameter of 8.7mm (*f*/6.3). Common glass BK7 and SF5 are used which can

give a strong index break at the doublet. We have three degrees of freedom in a cemented doublet, which can be used for focal length, spherical aberration and off sine condition (OSC). From the aberration point of view, the bending of a cemented doublet can yield zero spherical aberration position where OSC is nearly zero.

After the first beam splitter, there is the second lens system that forms the telephoto design. This consists of two lenses (L2 and L3), a positive meniscus lens and a negative meniscus lens, used to balance aberrations. There is then a second beam splitter, which allows for the extra camera to be added in the future. The whole leg was then optimised using Zemax with the wavefront error as the merit function. All aberrations were well corrected and the modulation transfer function was close to the diffraction limitation.

Beam Expander Design

The arrangement of the beam expander is nothing more than an inverted telescope. The lens L1, acts as the collimator and a negative lens is used to provide the beam expansion for the sake of compactness. The output diameter of the laser diode beam is 3mm so the required focal length of lens L4 is –18.96mm to expand the beam over the full aperture of the SLM. Since L1 is also part of the Fourier transforming system, the design optimisation is performed on L4 in Zemax. Construction the singlet lens using SF5 gives a spherical wavefront aberration error of only 0.03 waves over the full aperture.

Lens Tolerancing and Housing

It must be ensured that the lenses meet the requirements after tolerancing. Usually the lens is given a higher performance than needed during the design leaving an extra for tolerancing. The tolerances should not be too strict to give reasonable manufacturing costs both in optics and mechanics. Using Zemax, the tolerances are optimised and all optical components are given a tolerance on radius as 0.03 to 0.05mm (excluding plane surfaces which have 3 to 4 fringes), and on thickness and air space of lenses as 0.05mm. The decenter tolerance on the components is 0.03mm. These tolerances are practical to the manufacture's standard. Computer simulations show that with a normal distribution of these tolerances, 95% of lenses are within the limitation of the requirement of the FT lens

when the image distance is used to compensate some manufacturing errors. When the air spaces are used to compensate the manufacturing error in both optics and mechanics during the assembly, the performance of the lens system can be further improved. The system has been designed using a database of conventional lens elements in order to minimise the cost and construction time of the system.

For the accuracy and ease of manufacturing of the housing, the lenses were located in a lens barrel with metal spacers inserted to maintain the correct separation. All the components are aligned and mounted on a stiff aluminium board that is then attached to the PCB (ISA card). The arrangement of all optical components and their housing are shown on figure 4. A modulated diode laser system with temperature control was chosen, even though it has a large volume, for illuminating the SLM due to its high stability in intensity, wavelength and polarisation.

Experimental Results

The correlator system was run in binary mode with an input frame rate of 40ms and 36 templates were searched per input frame. The letter B was chosen as the input signal to be correlated and is shown in figure 5a). This was then autocorrelated and the example output captured by the CCD camera is shown in figure 5b).

The two correlation spots are expected from a binary filter. Binary filters are particularly sensitive to background clutter so in this example the system performed reasonable well. The resolution of the CCD2 camera is also limited to 128x128 pixels. To improve the performance of the filter in the presence of background clutter a different filter is required. The complex filter has not yet been implemented at full frame rate, but several test correlation results are shown using a CCIR camera output.

Figure 6 shows the autocorrelation of the letter A. The central spot is the DC term caused by unmodulated light from the surface of the SLM. The two spots on either side are the first and minus first order replications of the correlation spot.

To improve the noise discrimination ability of the system, a Wiener filter, $W(x,y)$, was implemented on the SLM [9,10],

$$W(x,y)=\left[\frac{R(x,y)^{*}}{\left|R(x,y)\right|^{2}+\left|N(x,y)\right|^{2}}\right] \qquad [6]$$

where $R(x,y)$ is the reference target and $N(x,y)$ is the noise term. Equation [6] is multiplied by the FFT of the input scene, $I(x,y)$, and this result was written to the SLM. The noise term was the mean power spectrum of several test images of clutter, although other models exist[9]. The noise term must remain static since the computational overheads of calculating equation [6] are large. With a constant $N(x,y)$ it can be calculated offline.

An example input is shown in figure 7a), an APC in background clutter. The correlation spot is shown in figure 7b) resulting from the cross correlation of the reference APC with this scene. The target is clearly picked out from the cluttered background. Another example is shown in figure 8a). In this case, the target is the fighter jet. A false target, a civilian jet, is shown in figure 8b). Figure 8c) shows the filter detecting the true target and figure 8d) shows the filter completely rejecting the false target.

Conclusions

This paper has discussed the design of a hybrid digital optical correlator. The electronic 2D FFT implementation and optical design have been discussed. Results of the correlator system operating with a binary filter and a fully complex Wiener filter have been shown. In both cases targets have been successfully identified.

Since the start of this project the available DSP chip sets have already doubled in speed. It may be expected that DSP technology will continue to improve with the provision of higher clock rates, larger amounts of on-chip memory and increased data transfer

bandwidths accompanied by falling costs. Thus, accurate and fast digital FFTs will become easier to implement. Recently we have run a 128x128 real to complex 2D FFT in 100ms on a 1.5GHz PC. These improvements will make possible the development of powerful hybrid systems with performance levels unachievable by either digital or optical signal processing hardware in isolation.

We gratefully acknowledge the Optical Systems Integration Programme of the Engineering and Physical Sciences Research Council (EPSRC) for their support of this research work.

References

1. Vander Lugt, "Signal detection by complex spatial filtering". IEEE Transaction on Information Theory, 10, pp 139-145, 1964.
2. T. Chao, H. Zhou, G. Reyes, "*512x512 High speed Greyscale Optical Correlator*" SPIE **4043** pp41- 45 (2000)
3. D. Carrott, G. Mallaley, R. B. Dydyk, S. A. Mills *"Third generation Miniature Ruggedized Optical Correlator (MROC) module"* SPIE **3386** pp39-44 (1998)
4. R.K. Wang, C.R. Chatwin**,** Lin Shang, "Synthetic discriminant function fringe - adjusted Joint Transform Correlator", Optical Engineering, 34(10), pp. 2935 - 2944, Oct 1995.
5. R. Cohn, "*Adaptive real-time architectures for phase-only correlation"* Applied Optics **32** (5) pp718-725 (1993)
6. D. Casasent, "General-purpose optical pattern recognition image processors", Proc. IEEE, 82(11), pp 1724-1734, 1994.
7. P.M. Birch, R.C.D. Young, D.M. Budgett, C.R. Chatwin, "*Fully Complex Optical Modulation using an Analogue Ferroelectric Spatial Light Modulator*" Optics Communications **175** pp 347-352 (2000)
8. Philip M. Birch, Rupert Young, David Budgett, Chris Chatwin, "*Two pixel computer generated hologram using a zero twist nematic liquid crystal spatial light modulator*" Optics Letters **25** (14) pp 1013-1015 (2000)

9. S. Tan, R. C. D. Young, D. M. Budgett, J. D. Richardson, C. R. Chatwin, "*Perfromance comparision of a linear parameteric noise estimation Wiener filter and non-linear joint transform correlator for realistic clutter backgrounds*" Opt. Comms **182** pp83-90 (2000)
10. R. K. Wang, R.C.D. Young, C.R.Chatwin, "*Assessment of a Wiener filter synthetic discrimination function for optical correlation*" Journal of Optics and Lasers in Engineering **22**(1) pp 33-51 (1995)

Process	**Time**
Input capture CCD camera frame rate	25Hz (40ms)
Complete real to complex FFT	Effectively 40ms with a pipeline delay
XOR operation for 128x128	10μs
Complex multiplication operation	~1ms
SLM data refresh rate	915Hz (1.1ms)
Peak detection camera rate	915Hz synchronised with SLM

Table 1

Table Captions

1. Frame rate of individual components within the system.

Figure Captions

Figure 1. Schematic of the hybrid digital/optical correlator.

Figure 2. The layout and connections of the electronic subsystem for the hybrid correlator

Figure 3. The layout and mount design for the optical subsystem for the hybrid correlator.

Figure 4. The mechanical design for the optics mount which are placed on the PCB board.

Figure 5. Binary correlation results. A) The input signal. B) The correlation plane.

Figure 6) Autocorrelation pattern of the letter A using a fully complex filter.

Figure 7) Weiner filter example. A) The target in clutter. B) The correlation plane.

Figure 8) Weiner filter examples. A) The target in clutter. B) A false target in clutter. C) The target's correlation plane. D) The false target's correlation plane.

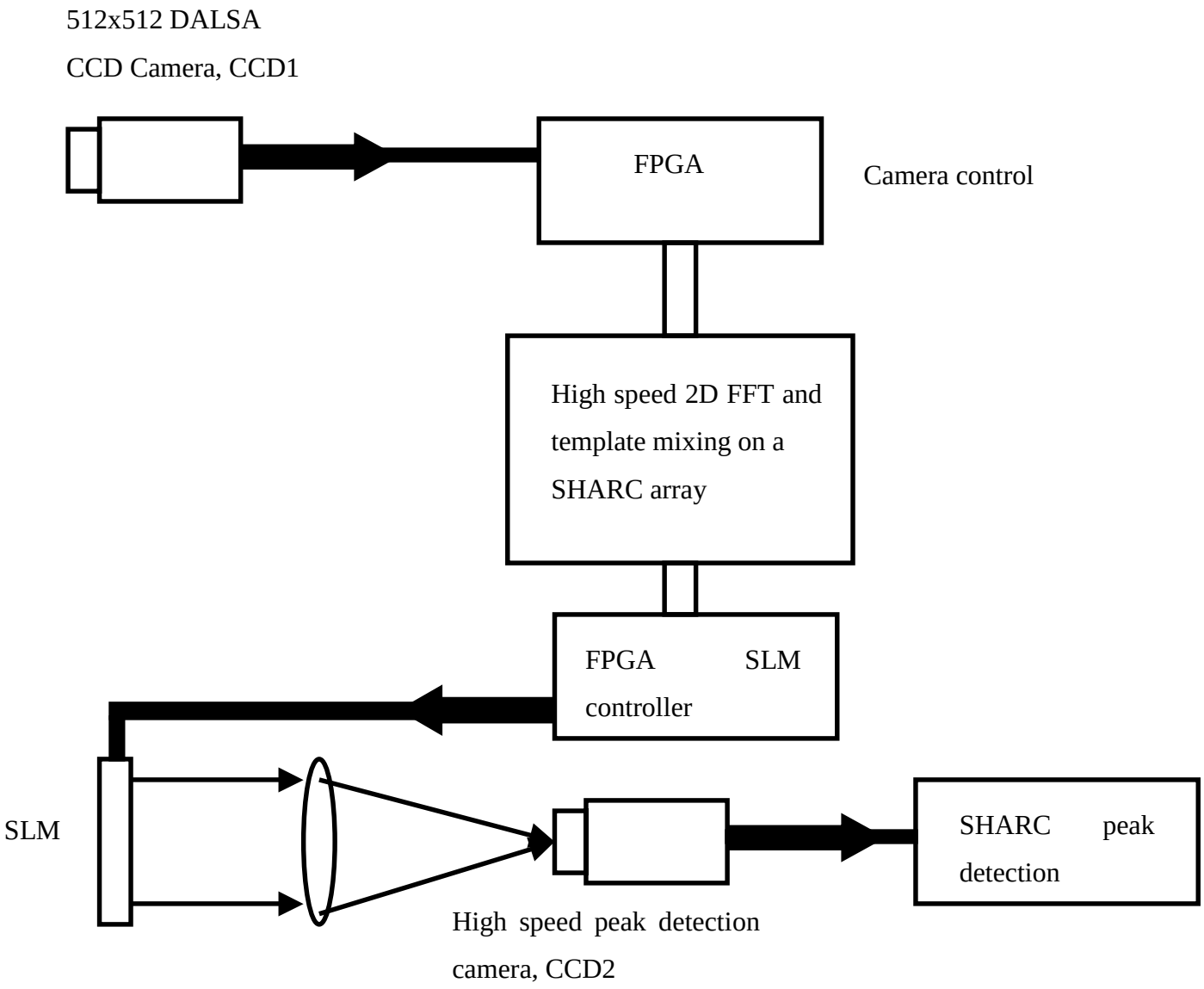
512x512 DALSA
CCD Camera, CCD1
FPGA
Camera control
High speed 2D FFT and template mixing on a SHARC array
FPGA SLM controller
SLM
SHARC peak detection
High speed peak detection camera, CCD2

Figure 1

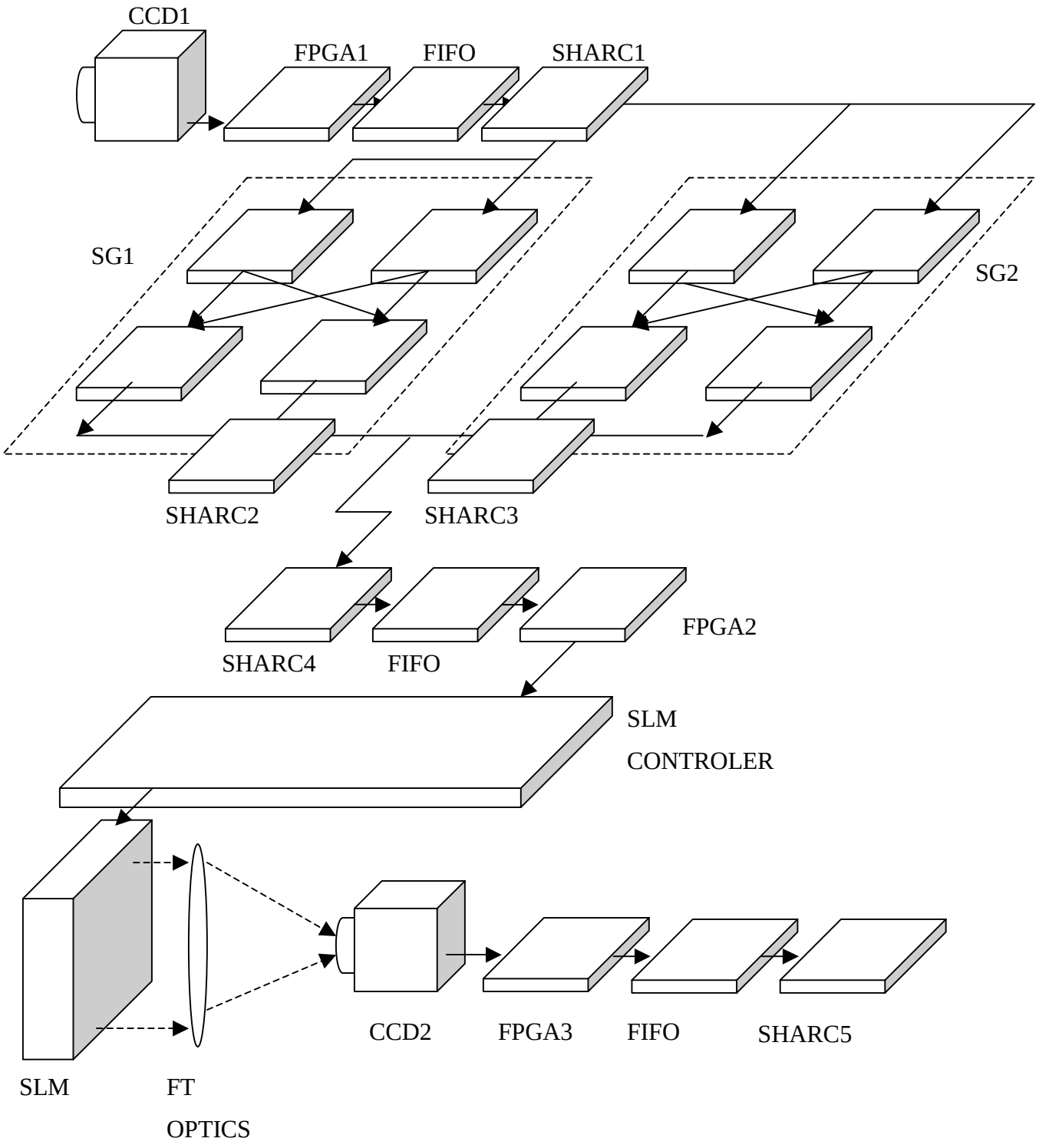
CCD1
FPGA1
FIFO
SHARC1
SG1
SG2
SHARC2
SHARC3
SHARC4
FIFO
FPGA2
SLM
CONTROLER
CCD2
FPGA3
FIFO
SHARC5
SLM
FT
OPTICS

Figure 2

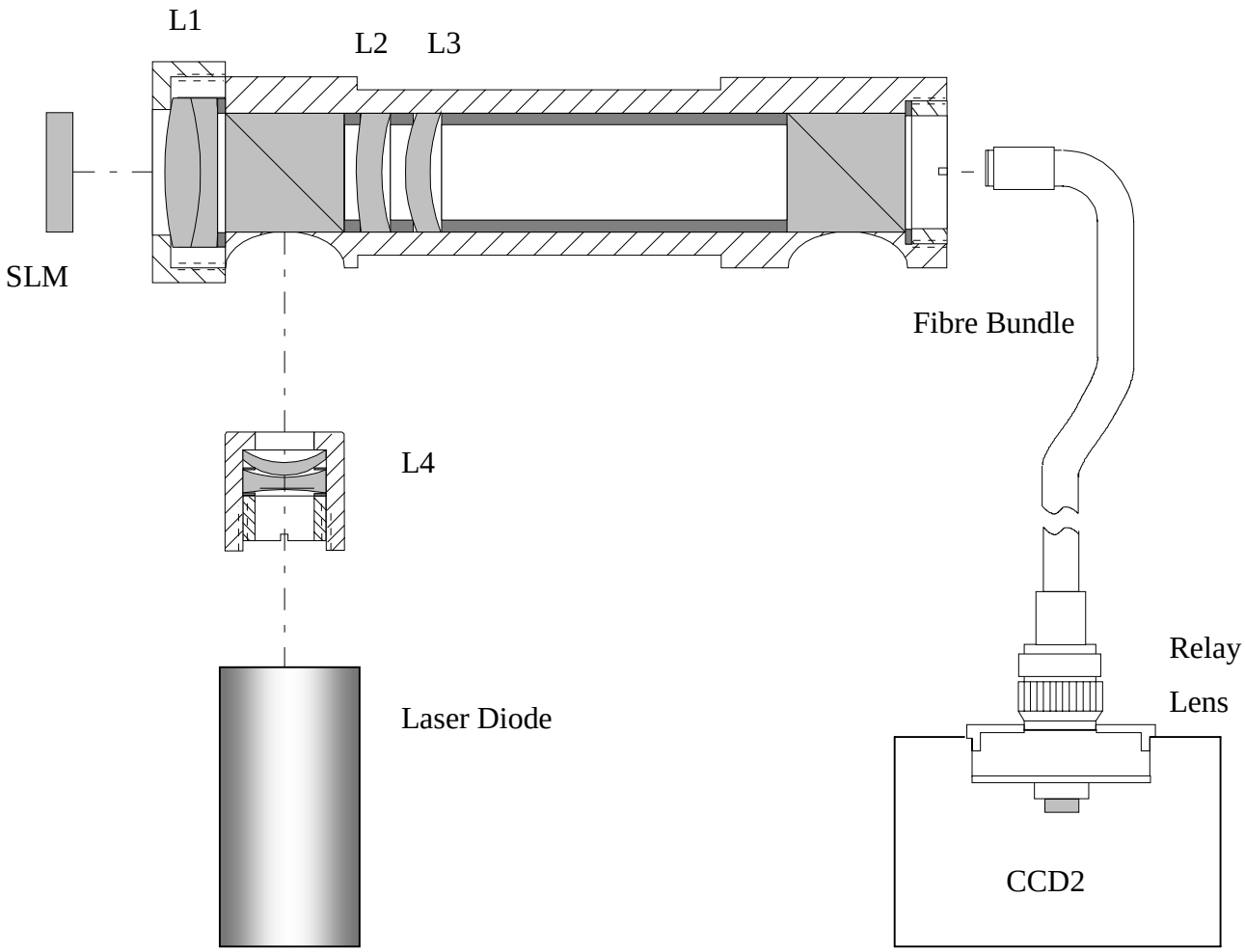

Figure 3

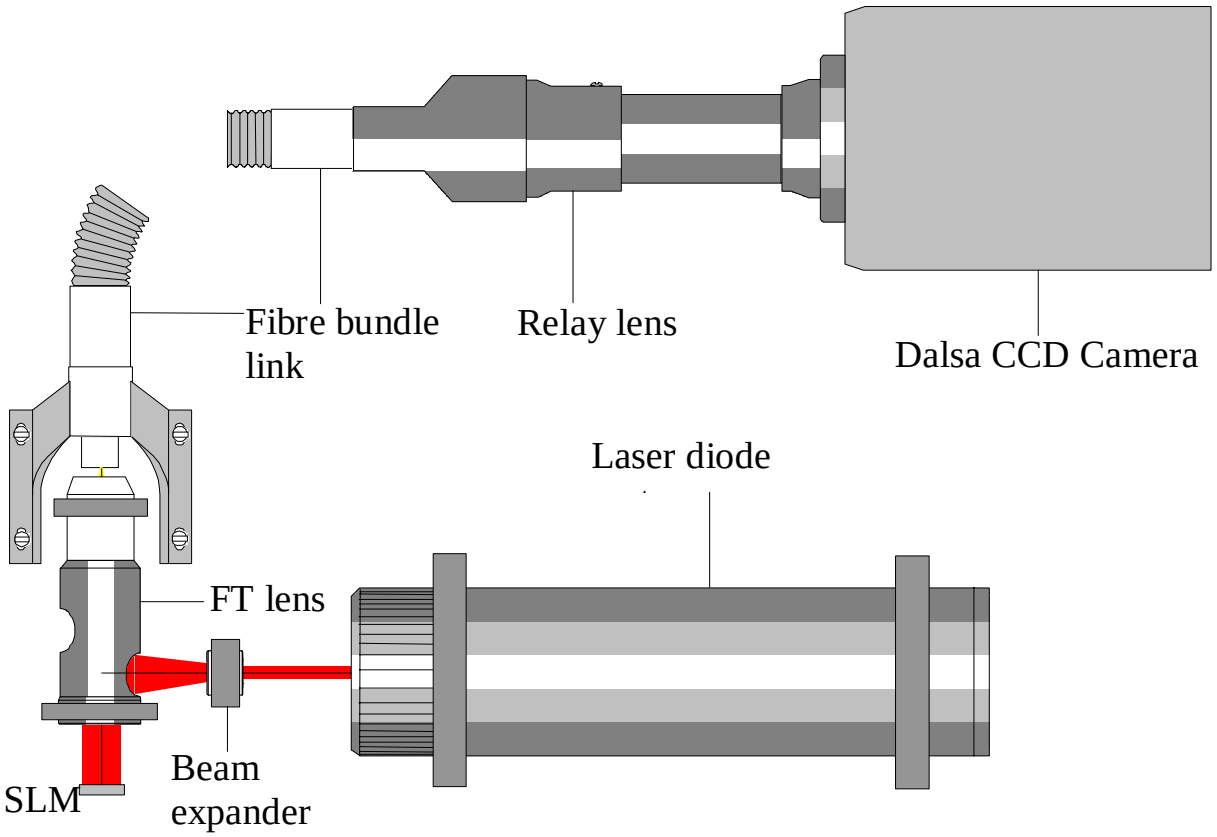
Fibre bundle link
Relay lens
Dalsa CCD Camera
Laser diode
FT lens
Beam expander
SLM

Figure 4

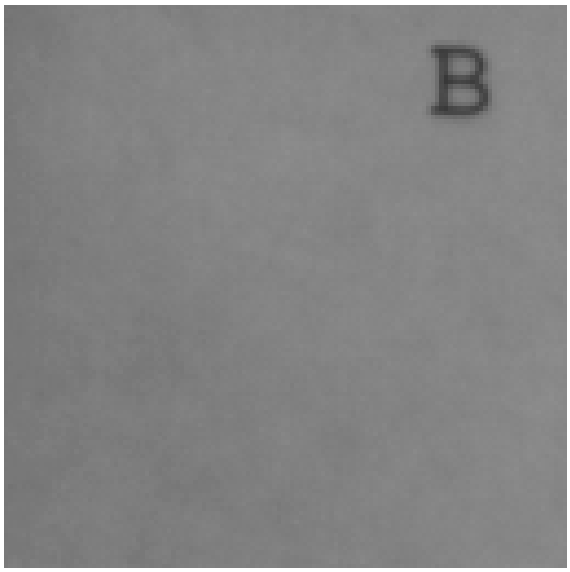

Figure 5 a)

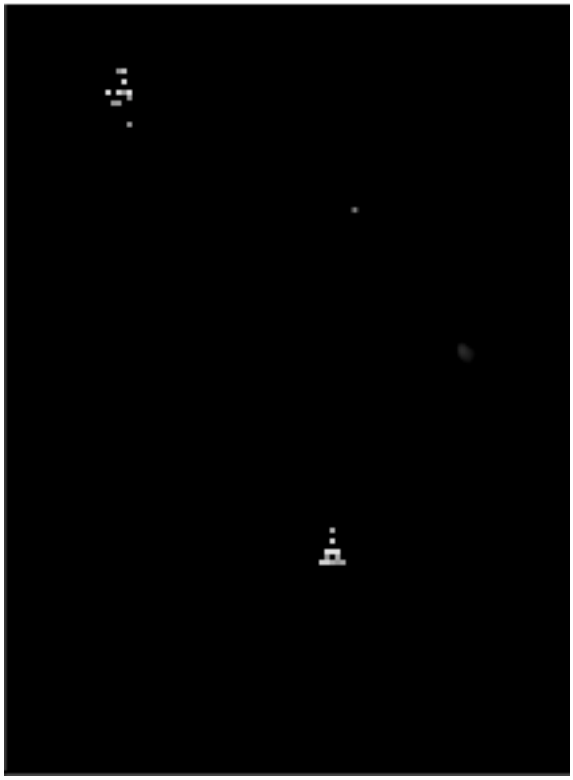

Figure 5 b)

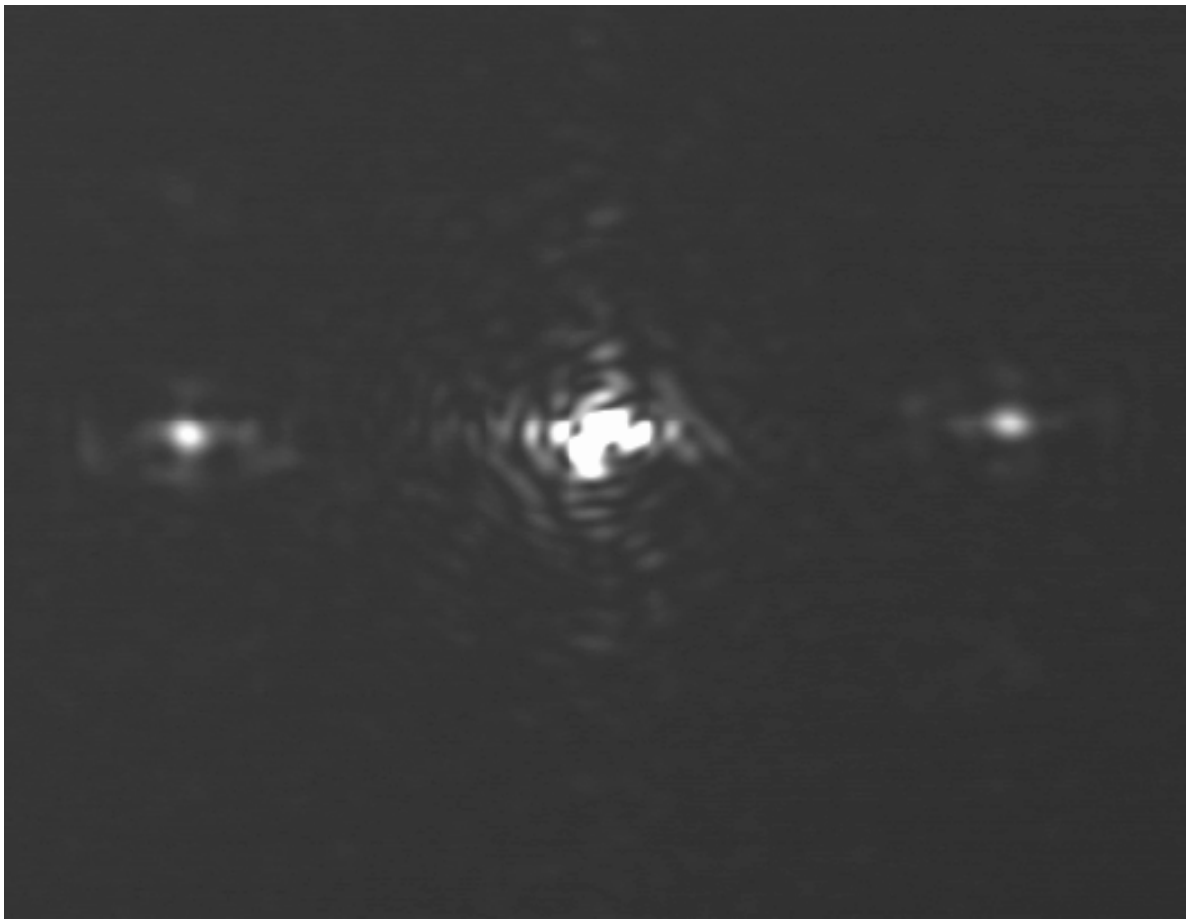

Figure 6

Figure 7a)

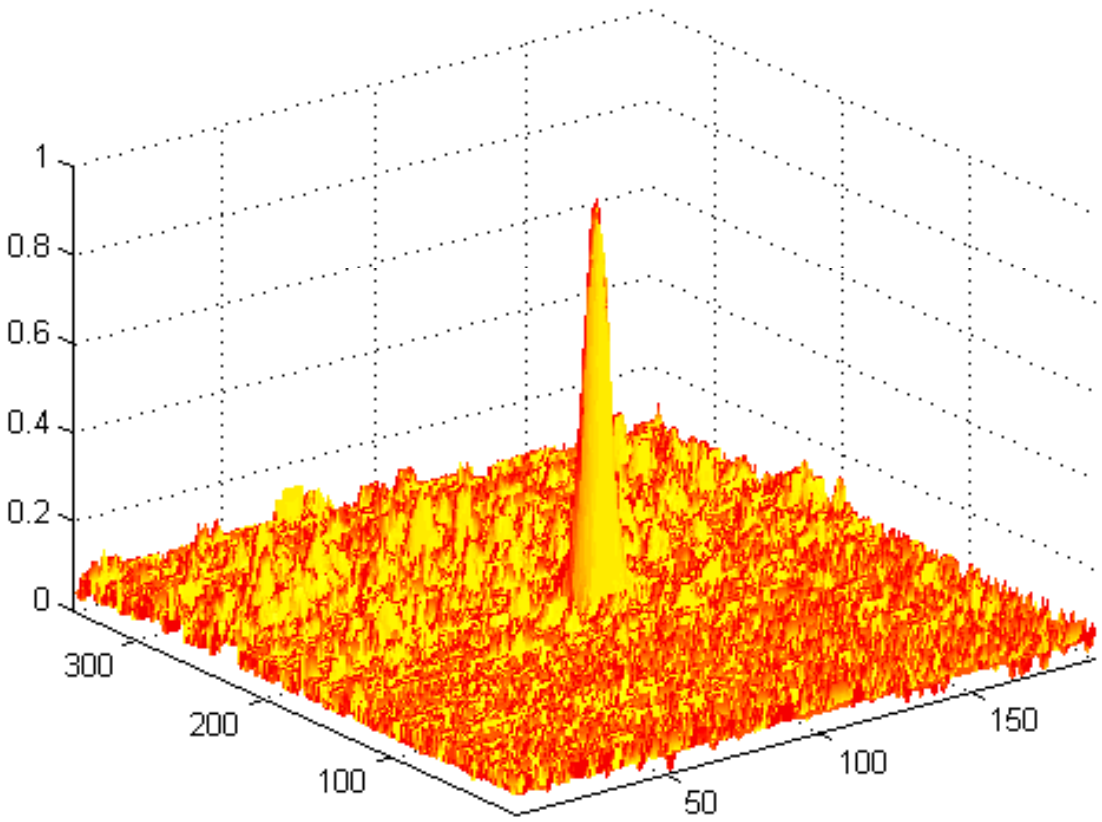

Figure 7b)

Figure 8 a)

Figure 8 b)

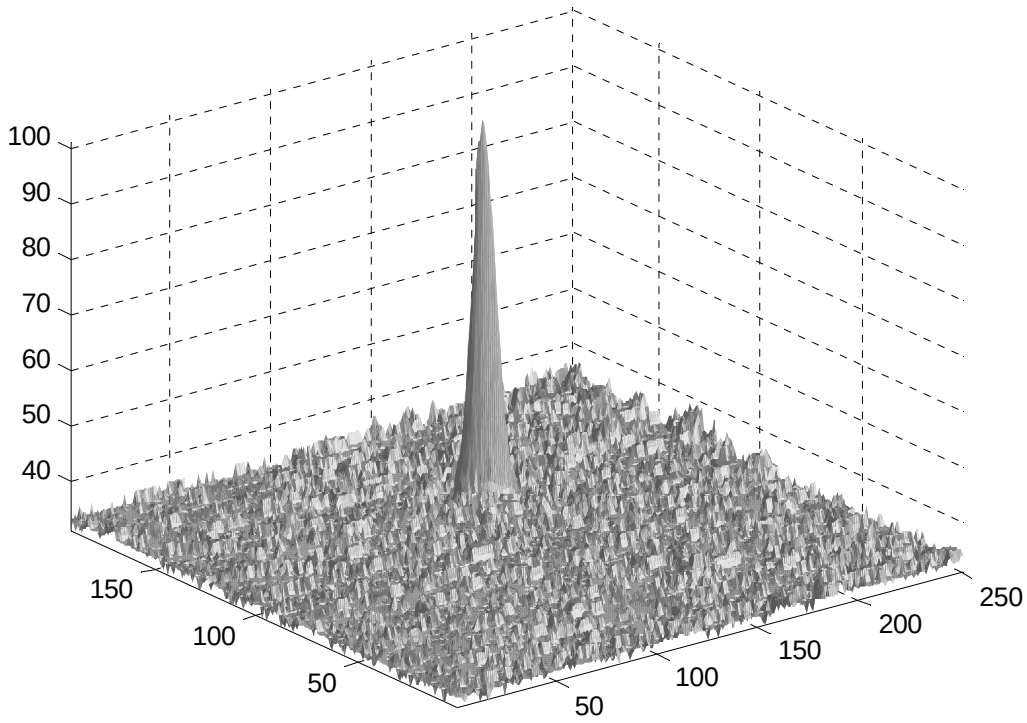

Figure 8 c)

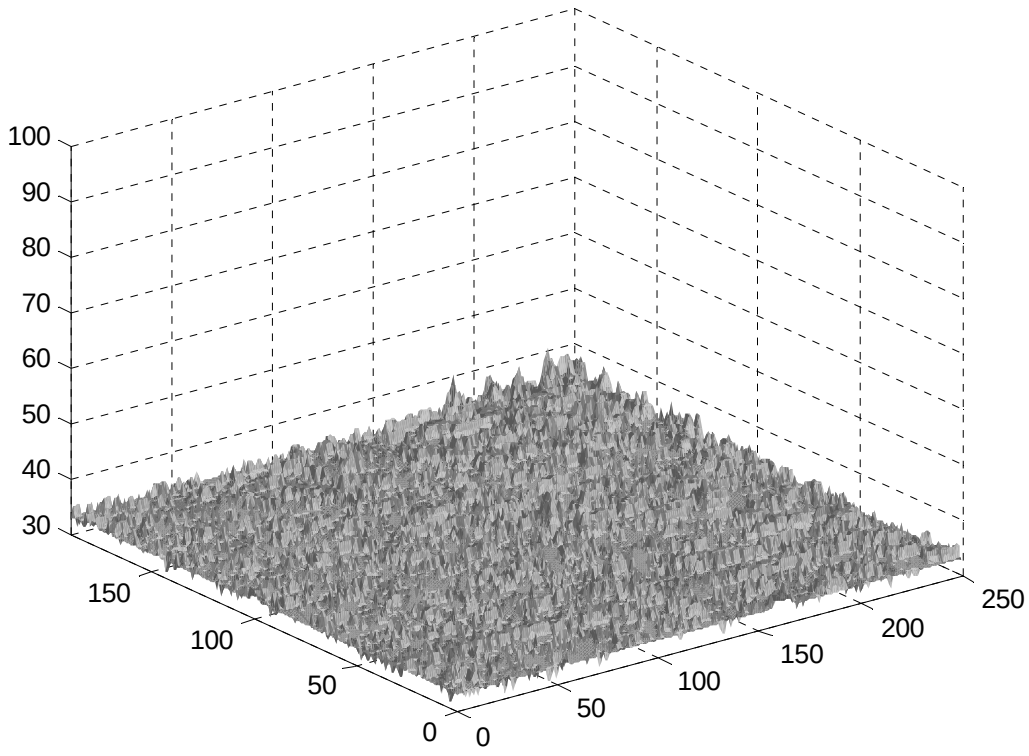

Figure 8 d)